

Chapter 12

Formulation optimization and characterization of
Olanzapine loaded Solid lipid nanoparticles – Effect of the
lipid matrix on the drug entrapment and invitro release

12.1 INTRODUCTION

Solid lipid nanoparticles (SLNs) have recently gained significant importance as potential alternate colloidal drug delivery system to liposomes, lipid emulsions and polymeric nanoparticles. The use of solid lipids is an attractive innovation which can provide the following advantages namely, the solid matrix of the lipid provides more flexibility in controlling the drug release and protects the encapsulated ingredients from chemical degradation and in comparison to liposomes SLN show slower degradation velocity *in vivo* because of its solid matrix. Another important advantage of SLN is the feasibility of scale up by high pressure homogenization (HPH) technique. SLN produced by HPH technique produces particles with an average particle size of less than 500nm and very low microparticle content.

SLN are usually free from the risk of acute or chronic toxicity because they are composed of physiological and biocompatible lipids. Various lipids including triglycerides (Heiati H et al., 1998; Bunjes H et al., 1996) and hard fat waxes (Westesen K et al., 1997; Cavalli R et al., 1992) have been used for the formulation of SLN. The choice of emulsifier and co emulsifier however depends on the route of administration and is more critical in parenteral delivery (Mehnert W et al., 2001).

Various research teams have studied the effect of lipid type on the final mean particle size of the SLN dispersions formed. Other factors like the velocity of lipid crystallization, the lipid hydrophilicity, influence on self-emulsifying properties on the shape of the lipid crystals, and hence the surface area were found to affect the final size of the SLN dispersions (Siekmann B et al., 1992). Till date only few attempts have been made to study the effect of lipid matrix on the drug entrapment, physical stability of the SLN dispersions.

Olanzapine is a psychotropic agent that belongs to the thienobenzodiazepine class and is indicated for acute and maintenance treatment of schizophrenia and related psychotic disorders (Bever KA et al., 1998). In this chapter, an attempt has been made to explore the effect of lipid type on the entrapment efficiency of the drug. For this, four lipids which are chemically different were selected namely glyceryl mono stearate (GMS) Precirol ATO 5 (PRE), glyceryl tristearate (GTS) and Witepsol E85 (WE 85). The effect of homogenization pressure and

homogenization cycle number on the size of nanoparticles were determined and optimized. The nanoparticles were characterized by differential scanning calorimetry, X-ray diffraction pattern and in vitro release profile was determined. Electrolyte induced flocculation test was performed to study the in vitro steric stability of the nanoparticles. Surface hydrophobicity was determined by Rose Bengal adsorption method. The nanoparticles were subjected for short term stability studies and the optimum stability conditions were determined.

12.2 MATERIALS AND METHODS

Materials

Olanzapine (OL) was received as a gift sample from Sun Pharmaceuticals, India. Poloxamer 407 was received as a free gift sample from BASF, Germany. Hydrogenated soya phosphatidyl choline (HSPC) was purchased from Lipoid GmbH (Ludwigshafen, Germany). Glyceryl mono stearate (mono ester of 16 carbon fatty acid stearic acid and glycerol) was purchased from Loba Chemie, India. Precirol ATO 5 (mono-, di- and triglycerides of palmitostearic acid with the diester fraction predominating) was obtained as a free gift sample from Colorcon India Limited. Glyceryl tristearate (tri glyceride derivative of 16 carbon fatty acid stearic acid and glycerol) and Witepsol E85 (hard fat in pastille form, consisting of mono-, di- and triglycerides of saturated fatty acids {10-18 carbon} of plant origin along with some amount of emulsifiers) were kindly provided by Sasol Chemicals, Germany. All other chemicals used in the study were of analytical grade. Water used in all the studies was distilled and filtered through 0.22 μm nylon filter before use.

Methods

Partitioning nature of olanzapine between the lipids and pH 7.4 phosphate buffer

Ten mg of OL was dispersed in a mixture of melted lipid (1 g) and 1 ml of hot pH 7.4 phosphate buffer (pH 7.4 PB) and shaken in a hot water (maintained at 10°C above the melting point of the lipid under investigation) bath using mechanical shaker for 30 min (Venkateswarulu V et al., 2004). The aqueous phase was separated from the lipid by centrifugation of the above mixture at 25,000 rpm for 20 min in a high speed centrifuge. The clear supernatant obtained after centrifugation was diluted suitably with 0.1N HCL and OL content was determined spectrophotometrically at 258nm against solvent blank.

The partition coefficient of olanzapine in lipid / pH 7.4 PB was calculated as following:

$$\text{Partition coefficient} = C_{\text{OLI}} - C_{\text{OLA}} / C_{\text{OLA}}$$

Where,

C_{OLI} = the initial amount of olanzapine added (10mg)

C_{OLA} = the concentration of olanzapine in the pH 7.4 PB.

Preparation and optimization of Solid Lipid Nanoparticles

Solid lipid nanoparticles (SLNs) were prepared by the slight modification of melt emulsification and high pressure homogenization method reported earlier (Reddy et al., 2006). Briefly, the lipid was melted and OL was dissolved to obtain drug-lipid mixture. Hydrogenated soya phosphatidyl choline (HSPC) was dissolved in about 0.3 ml chloroform and added to the above lipid- drug mixture. The mixture was warmed at about 60 to 65°C to evaporate the chloroform totally and the clear lipid melt containing HSPC was added to the hot aqueous surfactant solution preheated to 10°C above the melting point of the lipid, under high shear homogenization at 9500 rpm for 1 minute using Ultra Turrax (Ultra Turrax T-25, Germany) to result in a crude emulsion. The crude emulsion was subsequently homogenized in a high pressure homogenizer (Emulsiflex C5, Avestin, Canada) in a water bath maintained at 10°C above the melting point of the lipid. The nanoemulsion obtained was then cooled at room temperature to recrystallize the lipid back to the solid state. This resulted in the formation of drug entrapped SLN dispersions in an aqueous media. The SLN dispersions had a lipid content of 5%, stabilized by 1-3% surfactant (poloxamer 407). To study the entrapment efficiency the OL content with respect to the lipid matrix was varied from 2 to 5%.

Estimation of olanzapine in SLNs

The SLN in dispersion was aggregated by adding 0.1 mL of 10 mg/mL protamine sulfate solution, and the dispersion was centrifuged at 8000 rpm (Remi cooling centrifuge, Mumbai, India) to obtain the pellet. 0.1 ml of the supernatant was diluted suitably with 0.1N HCl and the free drug content was determined in a UV-visible spectrophotometer (Shimadzu, Japan) at 258 nm against suitable solvent blank. The pellet obtained was washed with distilled water and lyophilized after the addition of 2 parts by weight mannitol with respect to total lipid content of

the formulation. Accurately weighed lyophilized powder was dissolved in a mixture of methanol-chloroform (1:1); and suitably diluted with the same solvent mixture and analyzed in a UV-visible spectrophotometer (Shimadzu, Japan) at 276 nm against suitable solvent blank.

Characterization of SLN

A. Particle size and zeta potential measurements

Size and zeta potential of the SLN dispersions were measured by photon correlation spectroscopy (PCS) using Malvern Zetasizer Nano ZS (Malvern Instruments, UK). Size and zeta potential measurements were carried for both initial SLN dispersions and stability samples of SLN dispersions after appropriate dilution with distilled water.

B. Differential Scanning Calorimetry (DSC)

DSC analysis was carried out using a Differential scanning calorimeter (DSC-60, Shimadzu, Japan) at a heating rate of 10°C per minute in the range of 30°C to 250°C under inert nitrogen atmosphere at a flow rate of 80ml/min. Differential scanning calorimetry scans of plain OL, bulk GMS, bulk PRE, bulk GTS, bulk WE 85, OL loaded GMS SLN, OL loaded PRE SLN, OL loaded GTS SLN and OL loaded WE 85 SLN are shown in figure 12.4

C. X ray diffraction studies

Powder X-ray diffraction patterns were obtained using an X-ray diffractometer (Philips PW 1710) with Cu K α radiation generated at 30 mA and 40 kV. XRD diffraction patterns of plain OL, bulk GMS, bulk PRE, bulk GTS, bulk WE 85, OL loaded GMS SLN, OL loaded PRE SLN, OL loaded GTS SLN and OL loaded WE 85 SLN are shown in figure 12. 3

D. Determination of in vitro steric stability by electrolyte induced flocculation test

The electrolyte induced flocculation test was performed for the all the four SLN dispersions stabilized with 1.5% poloxamer 407. The effect of poloxamer 407 on the ability of the SLN to resist electrolyte induced flocculation was investigated by this test. Sodium sulphate solutions ranging from 0 M to 1.5 M were prepared in 16.7 %w/v sucrose solution (Subramanian N et al., 2003). An appropriate volume of SLN dispersion was made up to 5 ml using the sodium sulphate solutions of varying concentrations (0 M,0.3 M,0.6 M,0.9 M,1.2 M and 1.5 M) to obtain a final concentration of 1mg/ml lipid. The absorbance of the resulting dispersions was

measured within 5 min at 400 nm using a UV-Visible spectrophotometer (Shimadzu, Japan) against respective blank.

E. Determination of surface hydrophobicity by Rose Bengal adsorption method

Surface hydrophobicity of the nanoparticles was evaluated by the adsorption of the hydrophobic dye Rose Bengal on the particle surface (Gessner A et al., 2000). A fixed known amount of dye was added to the nanoparticle dispersions of various concentrations. Rose Bengal undergoes partitioning between the nanoparticle surface and the dispersion medium. The SLN in dispersion were aggregated by adding 0.1 mL of 10 mg/mL protamine sulfate solution, and the dispersion was centrifuged at 8000 rpm for 10 min. The fluorescence of free dye in the supernatant was measured by the absorbance at 548nm against suitable blank. Calibration plots were constructed for the measured absorbance values against drug concentration (Table 4.13; Chapter 4). The partition co-efficient (PC) was calculated as follows,

$$\text{Partition coefficient (PC)} = \frac{\text{Amount of Rose Bengal bound on the surface}}{\text{amount of Rose Bengal in the dispersion medium.}}$$

PC values obtained from the above formula for each nanoparticle concentration was then plotted against the total surface area (in $\mu\text{m}^2/\text{ml}$) of the nanoparticles. The slopes of the straight lines obtained were taken as a measure of the surface hydrophobicity.

F. Stability studies - Effect of temperature

Short-term stability studies were conducted on the various OL loaded SLN dispersions for a period of four months. The initial particle size and zeta potential of the OL loaded SLN dispersions were measured immediately after high pressure homogenization using Zetasizer (Malvern Zetasizer Nano ZS). Then the batch was stored in transparent colorless glass vials (USP type I) sealed and wrapped with black paper under different temperature conditions of 4°C (in a refrigerator) and 40°C (temperature regulated oven). Samples were withdrawn after 15, 30, 60, 90 and 120 days and were subjected to particle size and zeta potential measurements.

G. In vitro drug release

In vitro release of OL from the OL loaded GMS SLN, OL loaded PRE SLN, OL loaded GTS SLN and OL loaded WE 85 SLN were determined in both 0.1 N HCl and pH 7.4 PB. OL is freely soluble in 0.1 N HCl. In vitro drug release studies for all the four SLN dispersions upto 18 hours in 0.1 N HCl and 72 hours in PH 7.4 PB. The SLN dispersion was placed in a dialysis bag (cutoff molecular weight of 12000 Daltons, Himedia, India) and sealed at both ends. The dialysis bag was then dipped into the receptor compartment containing the dissolution medium. The release of OL from solution form in pH 7.4 PB containing 1% methanol (as control) through the dialysis bag was also studied using the same media. The dissolution media was continuously stirred at 100 rpm and maintained at $37 \pm 2^\circ\text{C}$. Samples were withdrawn at regular time intervals and the same volume was replaced with fresh dissolution medium. Samples withdrawn from 0.1N HCL were analyzed spectrophotometrically at 258 nm for OL content against a solvent blank. Samples withdrawn from pH 7.4 PB were analyzed spectrophotometrically at 276 nm for OL content against a solvent blank. All experiments were repeated thrice and the average values were taken.

12.3 RESULTS AND DISCUSSION

Partitioning nature of olanzapine between lipids and pH 7.4 phosphate buffer

Assessment of partition coefficient of drug in lipids would provide an idea about the entrapment of drug in the SLN. The partition coefficient was in the order of $\text{GTS} > \text{PRE} > \text{WE} > \text{85} > \text{GMS}$. The prerequisite to obtain adequate loading capacity of drug is high solubility of the drug in the lipid melt. In general, the solubility decreases after cooling down the lipid melt and might even be lower in the solid lipid. The presence of mono- and diglycerides in the lipid used as matrix material promotes drug solubilization (Muller RH et al., 2000). The chemical nature of the lipid is also important because lipids which form highly crystalline particles with a perfect lattice (e.g. monoacid triglycerides) lead to drug expulsion (Westesen K et al., 1997). Lipids which are mixtures of mono-, di- and triglycerides and lipids containing fatty acids of different chain length form less perfect crystals with many imperfections offering space to accommodate the drugs.

The difference in drug partitioning between the lipids can be explained as follows. OL is a hydrophobic drug with log P value of 2.199. Out of the four lipids investigated, GTS was able

to retain most amount of OL in its lipid matrix in comparison to the aqueous phase (partition value 2.77). This may be due to the fact that GTS is the most lipophilic of the four lipids and had higher affinity for OL. PRE gave a partition co-efficient value for OL (2.31). PRE being a mixture of mono-, di- and triglycerides and has more space i.e. more imperfections in its lipid matrix to accommodate the drug. WE 85 also being a mixture of mono- di- and triglycerides had a partition value (2.23) comparable with PRE. Further, the presence of emulsifiers in WE 85 may have played a role in the solubilization of OL in the lipid matrix leading to good partition. GMS gave the least partition value (1.91). The partition coefficient values obtained between the different melted lipids and phosphate buffer is tabulated in table 12.1.

The partition coefficient values obtained for the different lipids showed correlation with the entrapment efficiency of SLN. GTS SLN exhibited the highest entrapment of OL (94.31%) while the GMS showed the least entrapment efficiency (82.17%). There was no significant difference in the entrapment efficiency of PRE SLN and WE 85 SLN. These results reveal that an initial study of the partitioning nature of the drug between the melted lipid and aqueous media can give the formulator an idea regarding the possible entrapment in the SLN formulation.

| Lipid type | Ratio of OL in Lipid/Phosphate buffer pH 7.4 |
|------------------------------|--|
| Glycerol mono stearate (GMS) | 1.91 |
| Precirol ATO 5 (PRE) | 2.31 |
| Glycerol tri stearate (GTS) | 2.77 |
| Witepsol E 85 (WE 85) | 2.23 |

Table 12.1: Partition coefficient values for OL between the bulk lipid and phosphate buffer pH 7.4

Influence of homogenization pressure and homogenization cycle number

The optimum homogenization pressure was determined by passing the crude emulsion at different homogenization pressures such as 5000 to 10000 psi using 1.5% w/v poloxamer 407 as surfactant for all the four lipids. As the homogenization pressure was increased from 5000 psi to 10000 psi, a decrease in mean particle diameter of SLN dispersions was observed. The

optimum homogenization pressure was found to be 10000 psi for all the four lipids. Homogenization pressures above 10000 psi did not result in a significant decrease in the mean particle size diameter of the SLN dispersions. Thus 10000 psi was considered as the optimum homogenization pressure. This reduction in particle size is mainly due to the development of cavitation forces in the homogenization gap, which results in diminution of the lipid droplets to the nano size (Muller RH and Keck CM., 2004). The effect of the different homogenization pressures on the mean particle size diameter of the SLN dispersion is shown in figure 12.1.

The mean diameter of nanoparticles was measured for the lipid dispersions prepared using 1.5% w/v poloxamer 407 homogenized at 10,000 psi after different homogenization cycles. It was observed that, as the number of homogenization cycles was increased, the size of SLN dispersion decreased. The size distribution curve moved towards a narrow particle size distribution upto 3 cycles and a slight increase in size was observed after the 4th cycle, accompanied by a broad size distribution. The optimum number of homogenization cycles resulting in smaller sized nanoparticles was 3 cycles. The effect of the homogenization cycle number on the mean particle size diameter of the SLN dispersion is shown in figure 12.2.

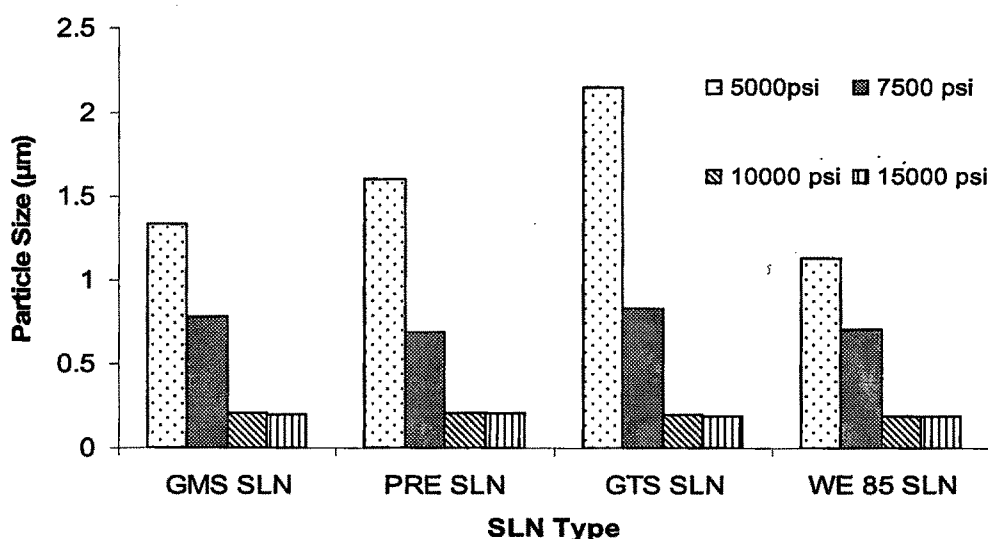


Figure 12.1: Effect of homogenization pressure on the size of solid lipid nanoparticles homogenized for three cycles

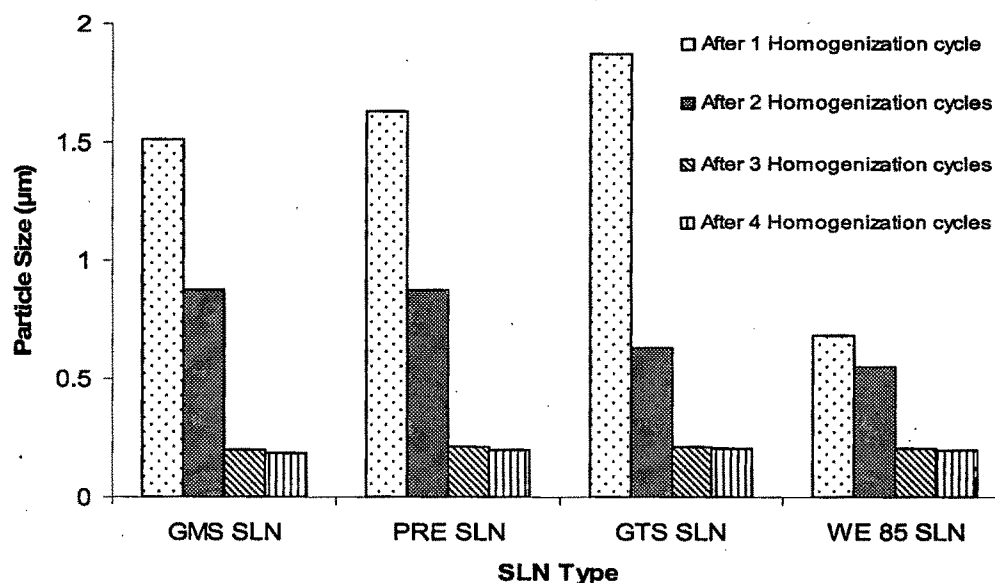


FIGURE 12.2: Effect of homogenization cycles on the size of solid lipid nanoparticles homogenized at 10,000 psi.

Optimization of Surfactant concentration

The main function of the surfactant is stabilization of the nanoparticles in the colloidal state and prevents particle size growth during storage. In addition to its role in stabilization, surfactants have also been shown to play a role in the crystallization behavior of the lipids. Bunjes and co-workers demonstrated that the crystallization temperature of nanoparticles made from triglycerides depends on the stabilizer, which can lead to homogenous or surface heterogenous nucleation (Bunjes H et al., 1996). The crystallization tendency of the particles increases with the length of the (saturated) hydrophobic chain of the stabilizer. The crystallization promoting effect of certain surfactants is believed to be caused by an ordering process of the surfactant molecules in the stabilizer layer. The type of stabilizer was also found to influence the rate of the polymorphic transitions. It was found that the stabilization with ionic surfactants leads to a slower transition than stabilization with nonionic surfactants (Bunjes H et al., 1996).

The mean diameter of OL loaded SLN dispersions stabilized with 0.5%w/v, 0.75%w/v, 1.0%w/v, 1.5%w/v and 2.0%w/v poloxamer 407 were measured. There was a gradual decrease in the particle size of the nanoparticles with increase in the surfactant concentration from 0.5%w/v to 1.5%w/v poloxamer 407. Increasing the surfactant concentration to 2.0% did not result in significant reduction in the size of the nanoparticles. Thus, the optimum surfactant concentration for all the four lipids investigated in this study was fixed as 1.5%w/v poloxamer 407. The choice of stabilizers is an important parameter to be considered in optimizing any nanoparticle formulation not only to control the particle size and stabilization of the dispersions but also to control the crystallization and polymorphic transitions (Bunjjes H et al., 1996). The mean particle size of the OL loaded SLNs stabilized with different concentrations of poloxamer 407 are shown in table 12.2.

| Nanoparticle type | Mean particle diameter (nm ± S.D.) | | | |
|-------------------|------------------------------------|---------------|---------------|---------------|
| | 0.5% w/v | 1% w/v | 1.5% w/v | 2% w/v |
| | Poloxamer 407 | Poloxamer 407 | Poloxamer 407 | Poloxamer 407 |
| GMS SLN | 776 ± 3.7 | 556 ± 3.4 | 198 ± 2.5 | 186 ± 2.7 |
| PRE SLN | 954 ± 2.3 | 600 ± 3.7 | 210 ± 1.8 | 198 ± 4.0 |
| GTS SLN | 895 ± 4.2 | 643 ± 3.8 | 208 ± 3.6 | 204 ± 3.4 |
| WE 85 SLN | 1062 ± 5.9 | 832 ± 5.0 | 194 ± 2.8 | 189 ± 2.6 |

TABLE 12.2: The mean particle diameter of the various olanzapine loaded solid lipid nanoparticles stabilized with the various concentrations of poloxamer 407

Entrapment efficiency of OL in the various SLN

Four different batches of nanoparticles were prepared by keeping the lipid concentration constant at 5%w/v and varying the concentration of olanzapine between 2%w/w, 3% w/w, 4% w/w, and 5% w/w w.r.t lipid. The results showed that increase in the concentration of the drug lead to the increase in drug entrapment efficiency of the SLN dispersions. The entrapment efficiencies obtained for the different lipids with the different drug loadings are tabulated in table 12.3.

The maximum drug loading possible was 4% w.r.t the lipid. Efforts to load more drug, for instance 5% lead to decrease in the entrapment efficiency. DSC and XRD studies showed the existence of drug in the lipid matrix in the amorphous state. This can be attributed to the fact that 4% drug loading led to a saturation of the lipid matrix and higher loading levels resulted in more of free drug rather than drug encapsulated inside the lipid matrix. In the present study, the order of entrapment was as follows: GTS SLN (94.31%) > WE 85 SLN (90.29%) > PRE SLN (87.07%) > GMS SLN (82.17%). Hence, it can be inferred that the nanoparticles prepared from mixed triglycerides are better alternatives to mono acid triglyceride nanoparticles.

There was good correlation between data obtained from the OL partition studies between the melted lipid and phosphate buffer pH 7.4 and the entrapment efficiency; GTS gave the highest partition value and the GTS SLN showed the highest OL entrapment efficiency. However GTS can the least partition value for OL and WE85 SLN gave the least entrapment efficiency. These results show that preliminary partition studies can give probable data regarding which lipid can give better entrapment when formulated as SLN.

| Concentration of OL w.r.t lipid (%w/w) | Entrapment efficacy (%) ± S.D | | | |
|---|-------------------------------|--------------|---------------------|--------------|
| | GMS SLN | PRE SLN | GTS SLN | WE 85 SLN |
| 2 | 80.31 ± 1.36 | 83.17 ± 1.08 | 87.02 ± 1.42 | 79.56 ± 1.22 |
| 3 | 82.63 ± 1.58 | 84.99 ± 1.44 | 90.54 ± 1.74 | 86.03 ± 1.66 |
| 4 | 86.87 ± 1.78 | 87.07 ± 1.76 | 94.31 ± 1.65 | 90.29 ± 1.39 |
| 5 | 75.04 ± 1.04 | 81.68 ± 1.52 | 85.07 ± 1.43 | 79.36 ± 1.20 |

Table 12.3: The entrapment efficacies of the different SLN dispersions

Characterization of SLNs formulations

Differential Scanning Calorimetry (DSC)

The crystalline structure of the nanoparticles can be assessed by differential scanning calorimetry (DSC). This is especially important when a drug exists in different polymorphic forms. The DSC results are tabulated in table 12.4. The DSC curve of OL (Figure 12.3) showed a melting endotherm at 193.05°C. This melting endotherm was not found as a sharp distinct transition in the thermograms of OL loaded GMS, PRE and WE 85 SLNs (Figure 12.3)

The melting endotherm was completely absent in the thermograms of OL loaded GTS SLN (Figure 12.3). This shows that the drug is mostly encapsulated inside the lipid matrix of the SLN.

Reduction in the melting point (m.p.) and enthalpy of the melting endotherm of the bulk lipid was observed when formulated as SLN (table 12.4). This can be attributed to the change in crystal lattice of the lipid after incorporation of OL and formulation as nanoparticles. These results are in agreement with those observed by Freitas and co workers (Freitas C and Muller RH., 1999). They observed that the crystallization behavior of Compritol SLN differed distinctly from that of the bulk lipid. These changes were due to the increased number of lattice defects in the lipid crystal. Small particle size of the SLN means high surface energy and this creates an energetically suboptimal state which leads to a decrease in the melting point. In the present study, incorporation of OL inside the lipid matrix might have lead to an increase in the number of defects in the lipid crystal lattice leading to a decrease in m.p. of the lipid in the final SLN formulations.

| Formulation | Enthalpy J/g ⁻¹ | Melting endotherm of lipid Peak (°C) |
|---------------------|----------------------------|---|
| Bulk GMS | -118.75 | 68.53 |
| Bulk PRE | -124.21 | 67.91 |
| Bulk GTS | -245.52 | 76.87 |
| Bulk WE 85 | -130.15 | 49.56 |
| OL loaded GMS SLN | -9.46 | 63.75 |
| OL loaded PRE SLN | -17.50 | 63.42 |
| OL loaded GTS SLN | -14.74 | 71.42 |
| OL loaded WE 85 SLN | -10.21 | 47.02 |

Table 12.4: Differential scanning calorimetry data of bulk lipids and olanzapine loaded SLN formulations.

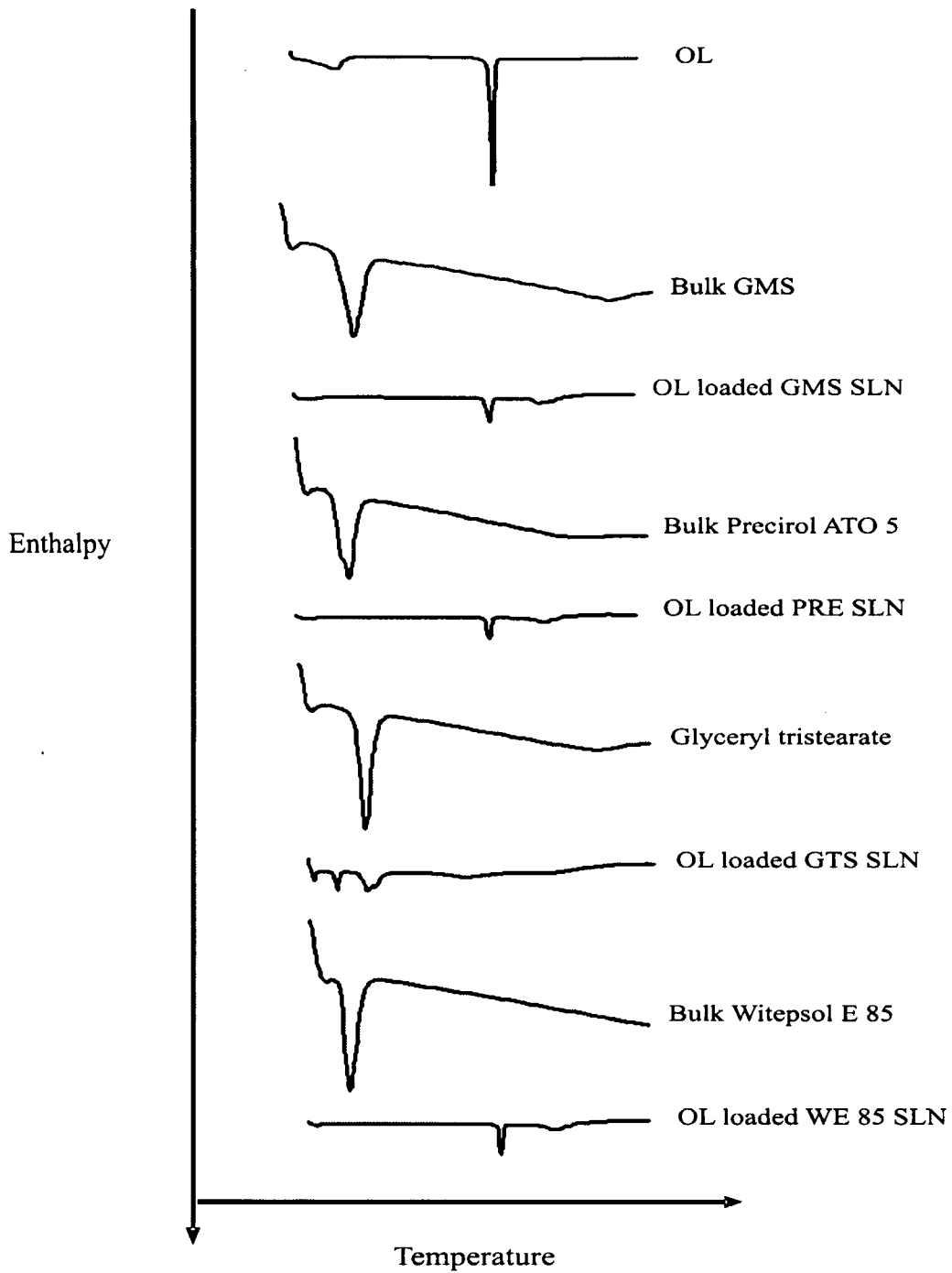


FIGURE 12.3: Differential scanning calorimetry curves of OL and the various OL loaded SLN formulations

X-ray diffraction patterns

Crystal diffraction has wide applications in the study of crystal forms (such as polymorphs, solvates, and salts). In the present study, comparison of the XRD patterns was done by considering the relative intensities of the diffracted peaks at a particular θ . The XRD data are tabulated in table 12.5. The XRD pattern of OL (Figure 12.4) shows a principal peak at angle $8.535^\circ 2\theta$. All the four lipids had the principal peak at around the same 2θ ($19.300^\circ 2\theta$). In the OL loaded SLN formulations, the principal peak of OL were absent in all the four OL loaded SLN formulations (Figure 12.4); further, the principal peak of the lipid did not shift. However, there was a reduction in the intensity of the principal peak in all the four SLN formulations. This may be attributed to the incorporation of OL in between the crystal lattice of the lipid leading to change in the crystallinity of the OL loaded SLN. These values complement the DSC data and clearly indicate the possible change in crystallinity of the lipid after OL incorporation and formulation.

| Formulation | Angle [2θ] | Peak intensity [counts] |
|---------------------|-------------------------------------|--------------------------------|
| Olanzapine | 8.535 | 1011 |
| Bulk GMS | 19.460 | 1490 |
| Bulk PRE | 19.390 | 1190 |
| Bulk GTS | 19.300 | 2550 |
| Bulk WE 85 | 20.995 | 2560 |
| OL loaded GMS SLN | 19.205 | 339 |
| OL loaded PRE SLN | 19.145 | 655 |
| OL loaded GTS SLN | 23.895 | 1056 |
| OL loaded WE 85 SLN | 23.905 | 912 |

TABLE 12.5: X ray diffraction data of bulk lipids and olanzapine loaded SLN formulations.

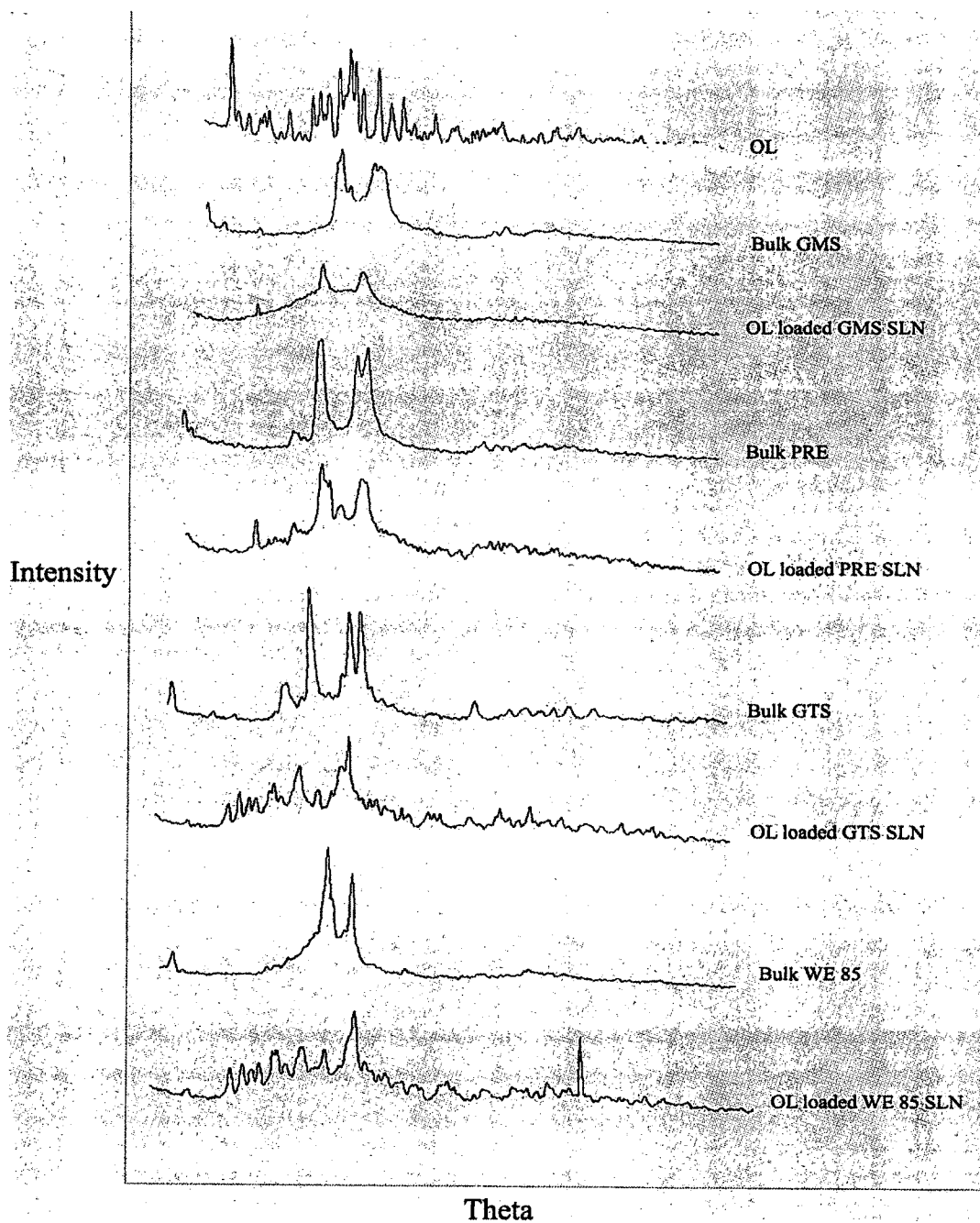


FIGURE 12.4: X – ray diffraction pattern of OL and the various OL loaded SLN formulations

Determination of in vitro steric stability by electrolyte flocculation test

The effect of poloxamer 407 on the ability of the nanoparticles to oppose electrolyte induced flocculation was investigated by this test. Coating the particulate systems with hydrophilic surfactants provide steric stability by rendering a hydrophilic surface, which in turn reduces the binding of serum opsonins and also cells of the reticuloendothelial system (Huang SK et al., 1993). Addition of electrolyte compresses the electrical double layer around the particle. This results in flocculation of the particles with a corresponding increase in optical turbidity of the particle dispersion which can be measured by the absorbance of the dispersion at 400nm. The scattering of the sample increased by the inverse 4th power of the wavelength of the incident light, and hence authors used a lower wavelength (400nm) was used for the measurements (Subramanian N and Murthy RSR., 2003).

In the present investigation, the nanoparticle formulations stabilized with 1.5%w/v poloxamer 407 showed a gradual increase in the flocculation as the concentration of electrolyte (sodium sulphate) was increased. All the four SLN dispersions showed signs of flocculation when the concentration of sodium sulphate was increased above 0.6M. Beyond this concentration, a sharp increase in the flocculation was observed. The results are given in figure 12.5.

Reddy and co workers studied the effect of various concentrations of poloxamer 407 on the in vitro steric stability of etoposide loaded GMS SLN and PRE SLN (Reddy LH and Murthy RSR., 2005). They observed nanoparticle agglomeration on the addition of just 0.4M sodium sulfate. The authors explained this behavior due to the dehydration of the poly oxy propylene and poly oxy ethylene during emulsification and high pressure homogenization. However, nanoparticles stabilized with 3% sodium tauroglycocholate showed superior in vitro steric stability in the presence of flocculating agent.

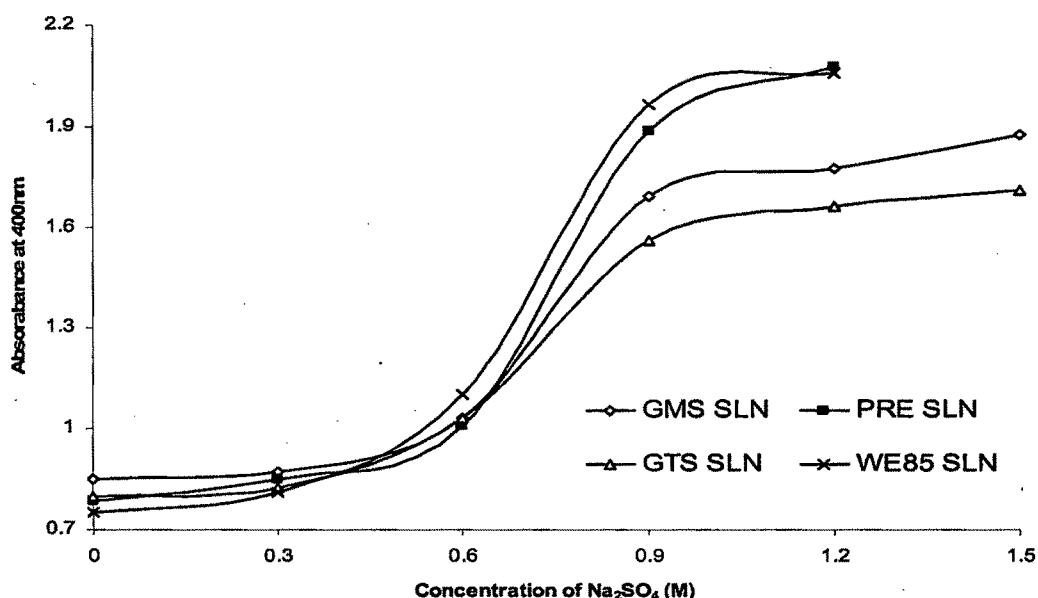


FIGURE 12.5: Steric stabilization effect of the various OL loaded SLN formulations. The nanoparticles were stabilized by 1.5% w/v of Poloxamer 407.

Determination of surface hydrophobicity by Rose Bengal adsorption method

The slope of the straight line obtained after plotting total surface area (in $\mu\text{m}^2/\text{ml}$) of the nanoparticles and partition value obtained for Rose Bengal were used to calculate the surface hydrophobicity; steeper the slope higher the surface hydrophobicity. Results are shown in figure 12.6.

The slopes i.e. the surface hydrophobicity obtained were in the order of GTS SLN (0.0457) > PRE SLN (0.0432) > WE 85 SLN (0.271) > GMS SLN (0.0207). Gessner and co-workers reported that the decrease in surface hydrophobicity is accompanied with a decrease in the quantitative amount of adsorbed proteins (Gessner A et al., 2000). Qualitative changes in the protein adsorption patterns were observed. However, they also confirmed that not only surface hydrophobicity, but also the functional groups present on the particle surface affects the protein adsorption. The poloxamer block copolymers are synthetic copolymers of ethylene oxide (EO; hydrophilic part) and propylene oxide (PO; hydrophobic) with a molecular weight

of around 11500. Poloxamer 407 has 64% of EO part and 36% of PO part with a HLB value of 18-23. Carstensen and co-workers observed that the hydrophobicity of nanoparticles decreased with an increase in the polyethylene oxide chain length of the poloxamer grade used for surface stabilization (Cartensen H et al., 1991).

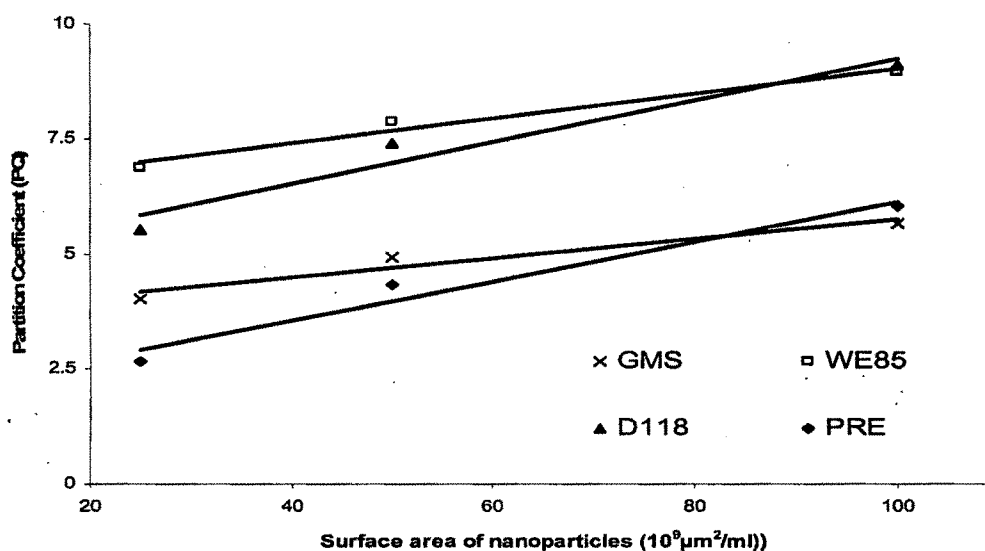


FIGURE 12.6: Plot of the partition coefficient (PC) versus the total surface area of the nanoparticles. The nanoparticles were stabilized by 1.5% w/v of Poloxamer 407.

Stability Studies

Effect of temperature on particle size

The particle size of the SLNs prepared from the different lipids immediately after production was not significantly different. However, their stabilities at different temperatures varied. The particle size was found to increase with storage as a result of particle aggregation. Mean particle diameter of the OL loaded GTS SLN stored at 40°C increased from $198 \pm 7.11\text{nm}$ to $908 \pm 8.64\text{nm}$ in 120 days, whereas for the OL loaded GTS SLN samples stored at 4°C, increased from the initial size of $198 \pm 7.11\text{nm}$ to $728 \pm 4.77\text{nm}$ (Figure 12.7). Another observation was the formation of rigid gel in the stability samples of OL loaded GMS SLN stored at 4°C after 15 days. Samples kept at 40°C did not gel. Further, a clear drug phase

separation was observed in OL loaded GTS SLN formulations. A thin layer of solid was found to sediment at the base of the glass vial. Similar gelling and drug phase separation was also observed by Westesen and co-workers during their study on the stability of phospholipid / tyloxapol trimyristin, Witepsol H42 and Witepsol H35 nanoparticles (Westesen K et al., 1997). The authors proposed that the gel formation is due to the difference in property of the colloidal lipid emulsions and suspension, and could be prevented by the use of a co-surfactant (Westesen K et al., 1997).

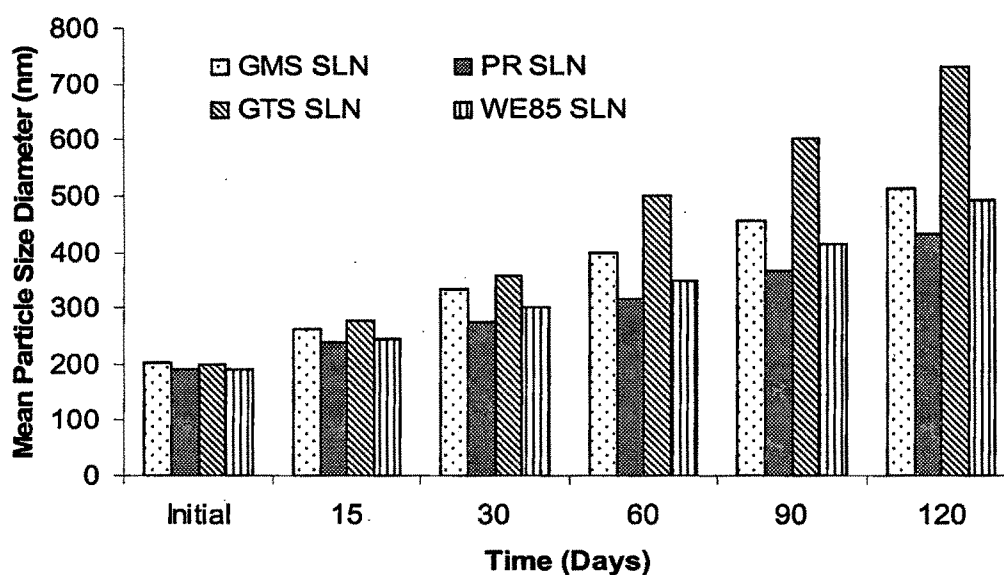


FIGURE 12.7: Mean particle diameter of the various OL loaded SLN formulations stored at 4°C after 15, 30, 60, 90 and 120 days.

Drug expulsion from the lipid matrix is a common problem during storage of SLN dispersions. Freshly prepared lipid dispersions are characterized by less ordered crystal lattice when compared to the bulk lipid. The lipid tends to crystallize to more perfect crystalline β -modifications which ultimately lead to drug expulsion (Muller RH et al., 2002). Jennings and co-workers observed that the SLN dispersions made from wax (cetyl palmitate and beeswax) were more stable when compared to glyceride nanoparticles showed particle growth and aggregation (Jenning V and Gohla S et al., 2000). Within glycerides, the best physical stability

was obtained for Dynasan, followed by Compritol. Imwitor is extremely unstable, and considerable particle growth takes place within a few days. Possibly, increasing amounts of partial glycerides like monoglycerides are responsible for this physical destabilization. These partial glycerides improve the surfactant film around the nanoparticles and thus prevent particle aggregation.

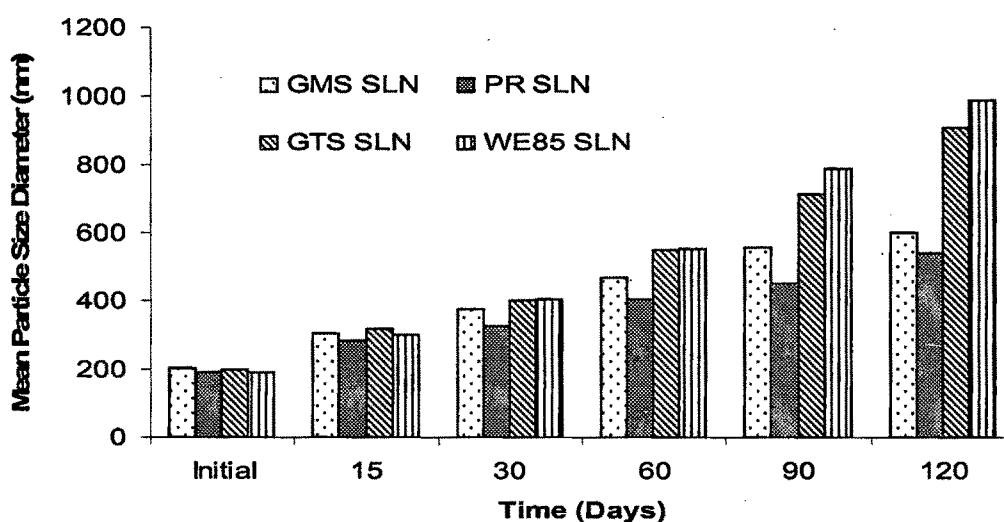


FIGURE 12.8: Mean particle diameter of the various OL loaded SLN formulations stored at 40°C after 15, 30, 60, 90 and 120 days.

A gradual particle size growth was observed increasing storage temperatures. Increase in the storage temperature is accompanied with an increase in the input energy which would destabilize of the nanoparticle dispersion. This input energy increases the kinetic energy of the particles which leads to increased particle - particle collision and ultimately results in aggregation. Aggregation of particles may lead to the partial destruction of the protective surfactant film covering the surface of the nanoparticle. This leads to exposure of the lipid which subsequently ends in bridging the particles. The surfactant used in this study, i.e. glycol copolymers (poloxamer) are characterized with reduced aqueous solubility at higher temperatures, which can lead to particle aggregation at higher temperatures. Cleavage of

hydrogen bonds between the hydrated polymer and water occurs at higher temperatures, leading to the formation of visible polymer aggregates (“cloud point”).

Effect of temperature on zeta potential

The zeta potential was found to drop with the increasing time duration of storage and increasing temperature. The changes in the zeta potential were more prominent for all the OL loaded SLN samples stored at 40°C when compared with those stored at 4°C (Figure 12.9). Increase in energy input to the SLN dispersion can lead to changes in the crystalline structure of the lipid (Freitas et al., 1998). Siekmann observed an increased β -modification during the storage of tripalmitate SLN (Siekmann B and Westesen et al., 1992). Crystalline re-orientation can result in changes of the charges on the particle surface (Nernst potential) and subsequently the zeta potential. In addition, different sides of a crystal can possess different charge density (e.g. aluminium silicates like Bentone™). Formation of long β crystals can take place during one-dimensional growth of a crystal (Sato K., 1988). This ultimately results in modification in the surface ratio of differently charged crystal sides and consequently the zeta potential changes.

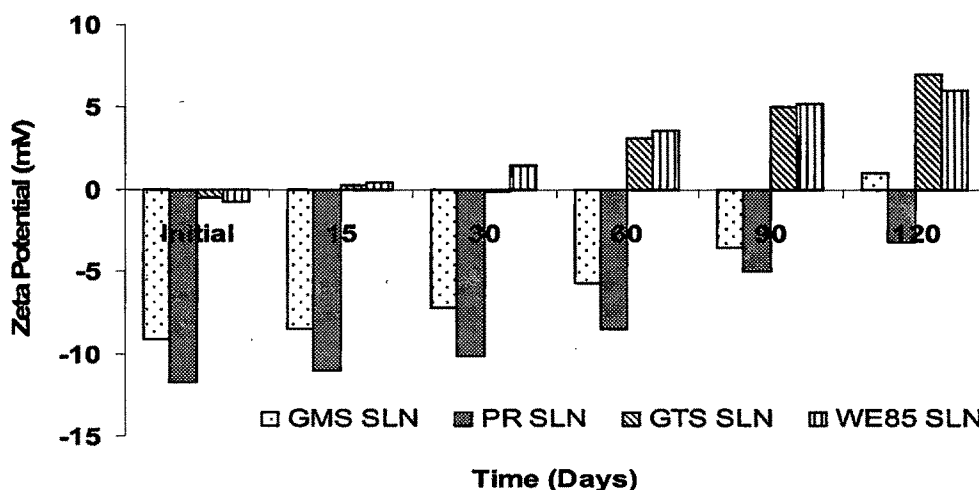


FIGURE 12.9: Zeta Potential values of the various OL loaded SLN formulations stored at 4°C after 15, 30, 60, 90 and 120 days.

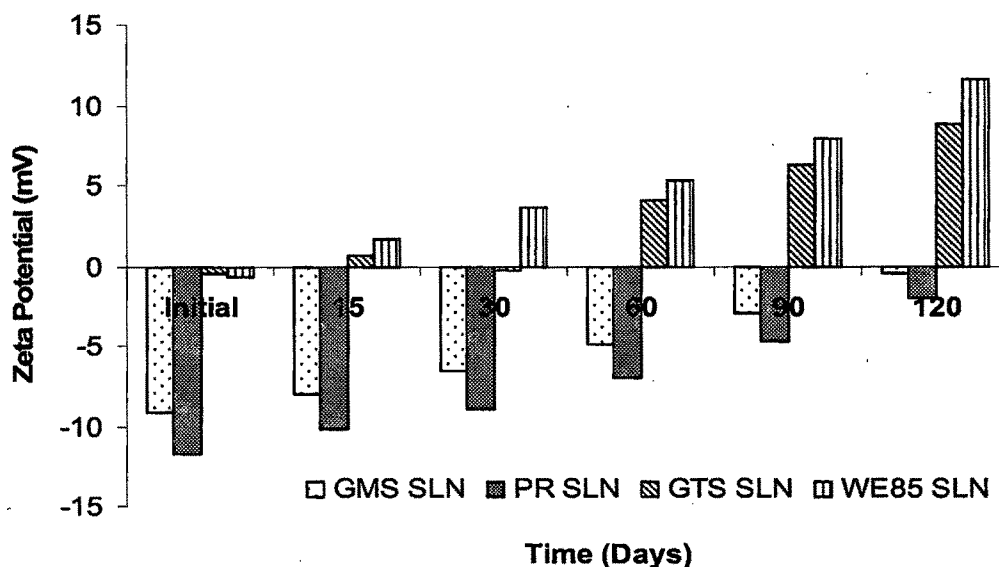


FIGURE 12.10: Zeta Potential values of the various OL loaded SLN formulations stored at 40°C after 15, 30, 60, 90 and 120 days.

In vitro release

The release of active substances from the matrix is influenced by the crystal structure of the lipid (Lukowski G et al., 2000). In vitro release of OL from the four SLN formulations was studied in 0.1N HCl (Figure 12.11) and pH 7.4 PB (Figure 12.12). The release profiles indicated that SLN dispersions showed a retarded release of the drug from the lipid matrix. The release profiles of all the four types of SLNs best fitted into the Higuchi equation (table 12.6). Comparative $t_{25} \pm S.D$ (time taken for 25% olanzapine to be released) t_{50} values (time taken for 50% olanzapine to be released) and t_{90} (time taken for 90% olanzapine to be released) of olanzapine solution and the various nanoparticle formulations in 0.1N HCl and phosphate buffer pH 7.4 is given in table 12.7 and 12.8 respectively.

All the nanoparticles exhibited initial burst release followed by sustained release. The initial in vitro burst release is probably caused by the drug adsorbed on the nanoparticle surface or precipitated from the superficial lipid matrix (Reddy LH and Murthy RSR., 2005). The

sustained release following the initial burst release is probably due to the diffusion of drug from the lipid matrix. The lipids investigated in this study are mostly long-chain fatty acids esters and are highly lipophilic (Hamdani J et al., 2003). GTS being the most lipophilic of the lipids presently studied gave the highest sustained release effect.

| SLN Type | 0.1N HCL | | pH 7.4 PB | |
|------------------------|---------------------------|--------|---------------------------|--------|
| | Higuchi (R ²) | Slope | Higuchi (R ²) | Slope |
| OL loaded GMS SLN | 0.9909 | 22.104 | 0.9928 | 11.193 |
| OL loaded PRE SLN | 0.9897 | 21.992 | 0.9901 | 10.573 |
| OL loaded GTS SLN | 0.9880 | 21.836 | 0.9909 | 9.896 |
| OL loaded WE 85 SLN | 0.9891 | 26.466 | 0.9965 | 15.462 |

TABLE 12.6: Kinetic evaluation of the OL release data for the different SLN formulations in 0.1N HCL and pH 7.4 PB

| Parameter | Time in minutes | | | | |
|-----------------|-----------------|---------------|---------------|----------------|---------------|
| | Plain OL | OL loaded | OL loaded | OL loaded GTS | OL loaded |
| | Solution | GMS SLN | PRE SLN | SLN | WE 85 SLN |
| t ₂₅ | 18.24 ± 1.09 | 69.01 ± 1.39 | 76.12 ± 1.80 | 115 ± 2.48 | 42.19 ± 1.31 |
| t ₅₀ | 35.42 ± 1.26 | 358.10 ± 3.44 | 415.14 ± 4.06 | 442.86 ± 3.35 | 237.06 ± 2.75 |
| t ₉₀ | 61.06 ± 1.44 | 946.52 ± 7.99 | 967.11 ± 6.12 | 1025.54 ± 9.53 | 541.39 ± 4.76 |

Table 12.7: Comparative t₂₅ ± S.D (time taken for 25% olanzapine to be released) t₅₀ values (time taken for 50% olanzapine to be released) and t₉₀ (time taken for 90% olanzapine to be released) of olanzapine solution and the various nanoparticle formulations. (Media: 0.1N HcL)

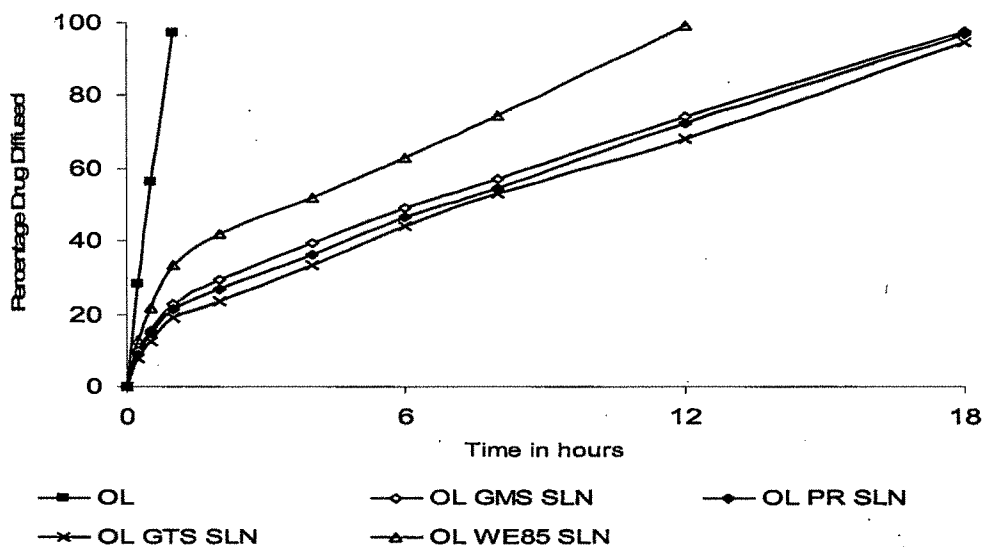


FIGURE 12.11: In vitro release of OL from plain OL solution and the various OL loaded SLN dispersions in 0.1N HCl.

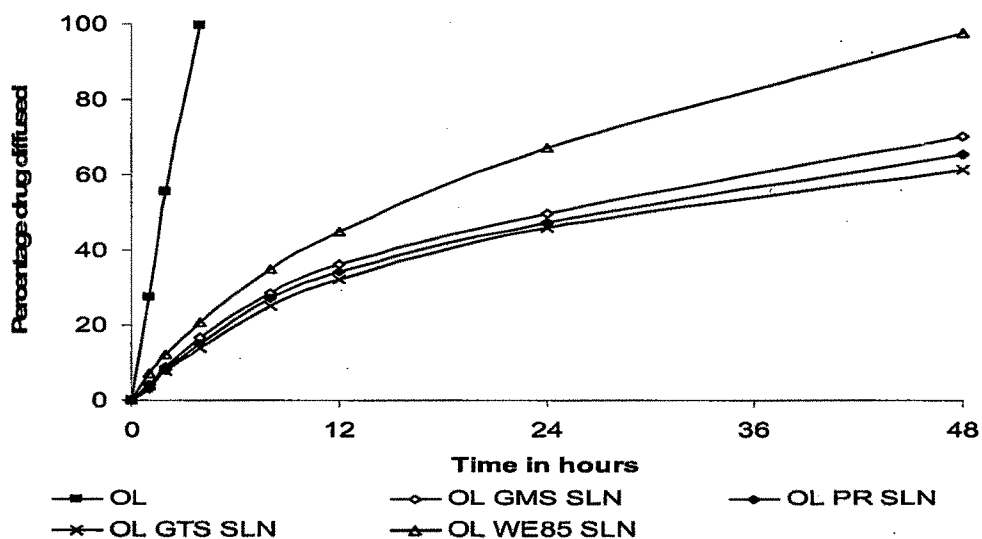


FIGURE 12.12: In vitro release of OL from plain OL solution and the various OL loaded SLN dispersions in phosphate buffer pH 7.4.

| Parameter | Time in hours | | | | |
|-----------|-------------------|-------------------|-------------------|-------------------|---------------------|
| | Plain OL Solution | OL loaded GMS SLN | OL loaded PRE SLN | OL loaded GTS SLN | OL loaded WE 85 SLN |
| t_{25} | 1.03 ± 0.09 | 7.11 ± 0.17 | 7.49 ± 0.24 | 8.05 ± 0.20 | 5.49 ± 0.15 |
| t_{50} | 2.15 ± 0.11 | 23.42 ± 0.56 | 26.60 ± 0.67 | 28.79 ± 0.70 | 13.05 ± 0.57 |

Table 12.8: Comparative $t_{25} \pm S.D$ (time taken for 25% olanzapine to be released) and t_{50} values (time taken for 50% olanzapine to be released) of olanzapine solution and the various nanoparticle formulations. (Media: phosphate buffer pH 7.4)

12.4 CONCLUSIONS

The present investigation demonstrates that preliminary partition studies of olanzapine between the molten lipid and pH 7.4 PB can give an idea about the achievable drug entrapment during formulation of lipid nanoparticles. The particle size of the nanoparticles can be controlled by varying process variables such as homogenization pressure and cycle number, and formulation variables, such as surfactant. The nanoparticles can be recovered in the powder form by lyophilization. The in vitro steric stability and surface hydrophobicity of the poloxamer 407 stabilized nanoparticles, coupled with sustained release in vitro characteristics created interest for further studies into the in vivo use of these nanoparticles as long circulating carriers in blood.

12.5 REFERENCES

- Bever KA, Perry PJ, Olanzapine: a serotonin- dopamine receptor antagonist for antipsychotic therapy, *Am J Health-Sys Phar.*, 1998, 55, 1003.
- Bunjes H, Westesen K, Koch MHJ, Crystallization tendency and polymorphic transitions in triglyceride nanoparticles, *Int J Pharm.*, 1996, 129, 159–173.
- Carstensen H, Muller BW, Muller RH, Adsorption of ethoxylated surfactants on nanoparticles. I. Characterization by hydrophobic interaction chromatography, *Int J Pharm.*, 1991, 67, 29-37.

Cavalli R, Gasco MR, Morel S, Behaviour of timolol incorporated in lipospheres in the presence of a series of phosphate esters, *STP Pharma Sci.*, 1992, 2, 514–518.

Freitas C, Muller RH, Effect of light and temperature on zeta potential and physical stability in solid lipid nanoparticle (SLN™) dispersions, *Int J Pharm.*, 1998, 168, 221–229.

Gessner A, Waicz R, Lieske A, Muller RH, Nanoparticles with decreasing surface hydrophobicities: influence on plasma protein adsorption, *Int J Pharm.*, 2000, 196, 245–249.

Hamdani J, Moes AJ, Amighi K, Physical and thermal characterisation of Precirol and Compritol as lipophilic glycerides used for the preparation of controlled-release matrix pellets, *Int J Pharm*, 2003, 260,47-57.

Heiati H, Tawashi R, Phillips NC, Drug retention and stability of solid lipid nanoparticles containing azidothymidine palmitate after autoclaving, storage and lyophilization, *J Microencapsul.*, 1998, 15, 173–184.

Huang SK, Martin FJ, Jay G, Extravasation and transcytosis of liposomes in Kaposi's sarcoma – like dermal lesions of transgenic mice bearing HIV Tat gene, *Am J Pathol.*, 1993, 143, 10-14.

Jenning V, Gohla S, Comparison of wax and glyceride solid lipid nanoparticles (SLN®), *Int J of Pharm.* 2000, 219–222.

Lukowski G, Kasbohm J, Pfliegel P, Crystallographic investigation of cetylpalmitate solid lipid nanoparticles, *Int J Pharm.* 2000, 196, 201–205.

Mehnert W, Mader K, Solid lipid nanoparticles Production, characterization and applications, *Adv Drug Del Rev.*, 2001, 47, 165–196.

Muller RH, Keck CM, Challenges and solutions for the delivery of biotech drugs – a review of drug nanocrystal technology and lipid nanoparticles, *J Biotechnology*, 2004, 113, 151–170.

Muller RH, Mader K, Gohla S, Solid lipid nanoparticles (SLN) for controlled drug delivery - a review of the state of the art, *Eur J Pharm Biopharm.*, 2000, 50, 161-177.

Muller RH, Radtke M, Wissing SA, Nanostructured lipid matrices for improved microencapsulation of drugs, *Int J Pharm.* 2002, 121-128.

Reddy LH, Murthy RSR, Etoposide-Loaded Nanoparticles Made from Glyceride Lipids: Formulation, Characterization, in Vitro Drug Release, and Stability Evaluation, *AAPS PharmSciTech*, 2005, 6 (2) Article 24. Available at: <http://www.aapspharmscitech.org>

Sato K, Crystallization of fats and fatty acids. In: Garti N, Sato K, eds. *Crystallization and Polymorphism of Fats and Fatty Acids*. New York: Marcel Dekker; 1988: 227–266

Siekmann B, Westesen K, Submicron-sized parenteral carrier systems based on solid lipids, *Pharm Pharmacol Lett.*, 1992, 1, 123–126.

Subramanian N, Murthy RSR, Use of electrolyte induced flocculation technique for an in vitro steric stability study of steric study of steric stabilized liposome formulations, *Pharmazie*, 2003, 59, 74-76.

Venkateswarlu V, Manjunath K, Preparation, characterization and in vitro release kinetics of clozapine solid lipid nanoparticles, *J Cont Rel.*, 2004, 95, 627– 638.

Westesen K, Bunjes H, Koch MHJ, Physicochemical characterization of lipid nanoparticles and evaluation of their drug loading and sustained release potential, *J Cont Rel.*, 1997, 48, 223-236.